



Application of 3D scanning and computer simulation techniques to assess the shape accuracy of welded components

Marianna Jędrych¹ · Damian Gorzkiewicz² · Mariusz Deja¹ · Marek Chodnicki¹

Received: 6 September 2024 / Accepted: 16 September 2024
© The Author(s) 2024

Abstract

While traditional measurement methods prove to be insufficient when facing more complex shapes and intricate challenges, increasingly efficient solutions are emerging in their place. 3D scanners in particular exhibit versatility. They clearly represent a useful tool in many fields with diverse requirements; thus, it is advisable to explore further areas of their potential applications, e.g., in quality control or reverse engineering. During our research, measurements were carried out on 40 welded elements using a caliper and on 11 other elements using the HandySCAN 700 Elite device by Creaform. The research was conducted at different stages of production, between subsequent operations. In addition, in the absence of interoperative nominal dimensions, a welding process simulation was performed in the Simufact Welding software. The simulation results were compared with actual deformations measured using a 3D scanner. The research enabled identification of the causes of excessive deformations and provided the basis for comparing the caliper with a modern laser device. A particular advantage of the scanner was demonstrated for complex issues requiring high flexibility and precise documentation of full geometry. The caliper proved to be more efficient only for quick execution of single, simple measurements at specific places. Incorporating the simulation in the Simufact Welding software into the analysis, allowed for a more precise validation of the planned technology. This solution presents a promising alternative to nominal models, particularly valuable when measurements are conducted between subsequent operations. Further research in this area is also recommended to enhance proposed methodology.

Keywords 3D scanning · Welding constructions · Quality control

1 Introduction

3D scanning is found to be useful in many fields including quality control and reverse engineering. This results in increasing popularity of modern measurement methods, which must enable the discretization of the geometry of various mechanical components, adapting to the requirements of a given field [1, 2].

Traditional measurement methods encounter difficulties and are unable to meet growing expectations and demands

of modern industry. Their limitations become increasingly apparent in the face of dynamic technological progress and the complexity of modern measurement tasks. Creating a virtual model based on collected dimensions is not an easy task, especially when dealing with objects of complex shapes or large sizes [3, 4]. Therefore, it becomes necessary to search for innovative measurement approaches that not only surpass traditional methods in terms of efficiency but also effectively respond to the variable and demanding nature of modern fields.

3D scanners are mobile devices that allow for contactless measurement process. They scan the entire area within their range, enabling data collection from multiple points simultaneously, which is an undeniable advantage of this method. However, 3D scanners encounter difficulties when measuring elements with reflective surfaces [5, 6], as well as deep, narrow holes and slots [7, 8]. A drawback of scanners operating based on the laser light technology is the requirement of reference points.

✉ Mariusz Deja
mariusz.deja@pg.edu.pl
Damian Gorzkiewicz
dgorzkiewicz@base.pl

¹ Faculty of Mechanical Engineering and Ship Technology, Gdańsk University of Technology, 11/12 Gabriela Narutowicza Street, 80-233 Gdańsk, Poland

² Base Group Sp. z o.o., Spacerowa 29 Street, 83-020 Koszwały, Poland

A particular advantage of non-contact solutions is the versatility of their application, from complex shapes [9] to large objects (for example, a 12-m-long yacht [10]), which would be difficult or even impossible to capture with contact measurements. With scanners operating on the “time of flight” technology, even entire buildings or geographical areas can be measured [11]. The application of scanning methods includes shipbuilding [12, 13], reproduction of car interior geometries for further numerical analysis [14], dental applications [15], implantology [5, 16], and many other fields.

3D scanners are becoming increasingly popular due to their speed and mobility, as well as the accuracy of measurements, which in many cases is sufficient. They also prove to be useful tools for dimensional and shape analysis of parts during quality control and reverse engineering [17]. In the context of reverse engineering, this modern method allows for the reproduction and analysis of objects with complex shapes. The idea of using 3D point clouds obtained with the aid of a handheld 3D laser scanner to identify various impact treatment levels applied to a steel weld toe was demonstrated in [18]. A good agreement was observed between the geometric parameters obtained from point cloud-based and silicon impression-based measurements. In [19], distortion of laser welded blanks (LWBs) was analyzed using 3D laser scanning to exploit distortion contribution plots to analyze spring back and wrinkling in forming processes. This inspection technique automatically rejected parts that have a negative effect on the conformity of parts and labor capacity of the machine and value chain in automobile industries. Profiles acquired from a 2-D laser scanner on square grooves in a multi-pass gas tungsten arc welding process were successfully used in [20] for automatic welding imperfections detection. As presented in [21], 3D laser scanning technology offers an opportunity to more accurately represent the weld geometry and accordingly perform fatigue assessment on more accurate representations of weld geometry.

Considering the above, in this research paper, 3D scanning was used to assess the shape accuracy of welded components. The research enabled identification of the causes of excessive deformations and provided the basis for comparing the caliper with a modern laser device. Actual deformations measured using a 3D scanner were compared with the simulation results from the Simufact Welding software. The proposed methodology offers an easily applicable solution for companies dealing with welding deformation, requiring only modest financial investment.

2 Study area

2.1 Contact and non-contact measurements

The research was conducted on two types of frames made of S355J2 steel. Both are assembled from flat bars and welded at the corners. The center of the frame, the space bounded by the flat bars, will be referred to as the eye. This paper will analyze one series of one-eyed frames with a flange (Fig. 1 on the left) and a part of the two-eyed series (Fig. 1 on the right), also, respectively, referred to as type 1 and type 2. In both cases, the focus was on the dimensions of the eye—its height h and width w .

The eye of type 1 frame consists of 4 flat bars, two short ones and two long ones, which will henceforth be, respectively, referred to as “K” and “P.” Measurements of 40 type 1 frames were carried out using a caliper at 4 stages of their production:

1. Measurements of the length of 160 flat bars (80 “K” and 80 “P”)
2. Measurements of frames after welding operation I
3. Measurements of frames after welding operation II
4. Measurements of frames after welding operation III

Fig. 1 On the left is type 1 frame; on the right is type 2 frame



The study of 11 type 2 frames was conducted using a 3D laser scanner and only included two stages:

1. Measurements of frames after welding operation I
2. Measurements of frames after welding operation II

2.2 Analysis in the Simufact Welding software

The absence of interoperative nominal dimensions posed a significant obstacle. It was impossible to accurately assess whether the obtained results met the expectations associated with the applied technology. While it is not possible to completely prevent deformations after welding processes, there are factors that can minimize or intensify them. To identify some of these factors, it was proposed to conduct numerical simulation in the Simufact Welding software.

The idea was to verify the effectiveness of the applied methodology when the flat bars subjected to welding would be ideal models. The obtained results will be compared with measurements of 11 scans in VXinspect, where the model of a flat bar assembly will serve as a reference. In this paper, an analysis of deformations will be presented only for welding operation I of type 2 frames.

3 Instruments and methodology

3.1 Contact measurements

For contact measurements, it was decided to use a caliper as a tool due to its availability and ease of use. The selected model, CDNBT by LIMIT brand, allowed for an accuracy of approximately 0.02 mm. A disadvantage of the caliper is its relatively high dependency of the accuracy and repeatability of results on the operator. Each flat bar had markings indicating three control points for height h and width w measurements of the eye after welding operations I, II, and III.

The obtained results were subjected to Statistical Process Control. The data was plotted on the individual moving range (I-MR) control chart from which Upper Control Limit for the Moving range (UCL_MR) was calculated. UCL_MR is a parameter that represents the predictability of the process. The higher the value, the more disturbed and unreliable the process is.

3.2 Non-contact measurements

Non-contact measurements were performed using the Creaform HandySCAN 700 Elite device along with the corresponding VXelements software. It is a handheld, portable device operating based on triangulation technology. The scanner generates 7 red crosses of laser light, enabling rapid digitization of the entire object. Additionally, this model

offers the option of using a single-ray line, which is useful for scanning holes, details, or other hard-to-reach areas. The accuracy of the HandySCAN 700 Elite reaches up to 0.03 mm, although it decreases as the size of the scanned object increases. The Creaform HandySCAN 700 Elite scanner is controlled through the compatible VXelements software, specifically VXscan. This software enables device calibration and guides the entire 3D scanning process. Control over parameters such as aperture value and resolution are available within VXscan, although the aperture value can also be adjusted directly using buttons on the device itself.

The scanning of one object took on average about 11 min and was conducted on a measurement table covered with reference points.

Each frame required two scans to be performed in two different positions. This allowed for capturing surfaces that were otherwise in direct contact with the table. This meant performing the first scan in one position, then flipping the object to expose the surface previously facing downwards, and performing the second scan. A 3D model is created by merging the two obtained meshes in the VXmodel software and then subjected to analysis in VXinspect.

The processed 3D models, after being imported into the VXinspect software, were properly prepared for conducting the inspection. The program allows referencing each part to the nominal CAD model. Due to the lack of nominal interoperative dimensions, the inspection of dimensions of the eye was carried out by comparing it to an automatically generated ideal rectangle.

3.3 Simulation in the Simufact Welding software

The simulation process required preparing meshes of models in the bdf file extension. Meshes of the flat bars were modeled separately, and their assembly was imported into the Simufact Welding software. The model was placed on the table (Bearing) and fixed (FixedGeometry), as illustrated in Fig. 2. These fixtures are not an exact representation of the actual fixtures; they are simplified in the form of cylinders establishing the dimensions of the frame's eye. Additionally, gravity acts on the entire assembly.

The selected steel grade from the library corresponds to both the base and consumable material. Although the welding wire differed, an approximation was used based on the similar chemical composition of both materials. Eight trajectories were plotted to represent the path of each welding bead in accordance with the frame's technical documentation. These trajectories can be observed in Fig. 2. in the form of black vectors based on red nodes of the mesh. The input data required by the software for the process simulation were current intensity, voltage, welding speed, and the deposition efficiency characterizing the welding method. These parameters were taken from the Welding Procedure Specification



(WPS). Moreover, the dimensions of the welding pool were also required by the software as input data for the simulation and thus estimated based on real industrial practice and experience. The analysis lasted for 2 min 30 s which covered both the simulation of eight welding beads and the process of cooling.

4 Results

4.1 Results of contact measurements

Due to the need to maintain data confidentiality, the dimensions of the eye will not be provided. From the Statistical Process Control (SPC) analysis, the UCL_{MR} values will be presented.

The obtained values of UCL_{MR} are summarized in Table 1 and Table 2. The first table contains information regarding the width of the eye, i.e., the length of the flat bar “K,” followed by the value of w measured from the front

and rear after welding operations I, II, and III. The second table presents analogous parameters, at the same stages, but concerning the length of the flat bar “P” and the height of the eye. The lowest value of UCL_{MR} was achieved for the flat bar “K,” while the highest was for the dimension w measured from the front after welding operation III.

It should be noted that 95% of the flat bars “P” are within tolerance, whereas among the flat bars “K,” 82.5% meet the criteria. Meanwhile, the UCL_{MR} result clearly shows that the repeatability of the process for shorter flat bars (“K”) is lower than for longer flat bars (“P”). This indicates a situation where the entire range of achieved dimensions of plate “K” is shifted, resulting in a greater number of errors despite the higher predictability of the process.

A different relationship between UCL_{MR} for width and height of the eye can be observed already after welding operation I. After this operation, the width dimension of the eye becomes less repeatable and predictable than its height. In general, UCL_{MR} increases after almost every process. This is a result of the applied welding processes and the

Fig. 2 The model of the welded component in the Simufact Welding software

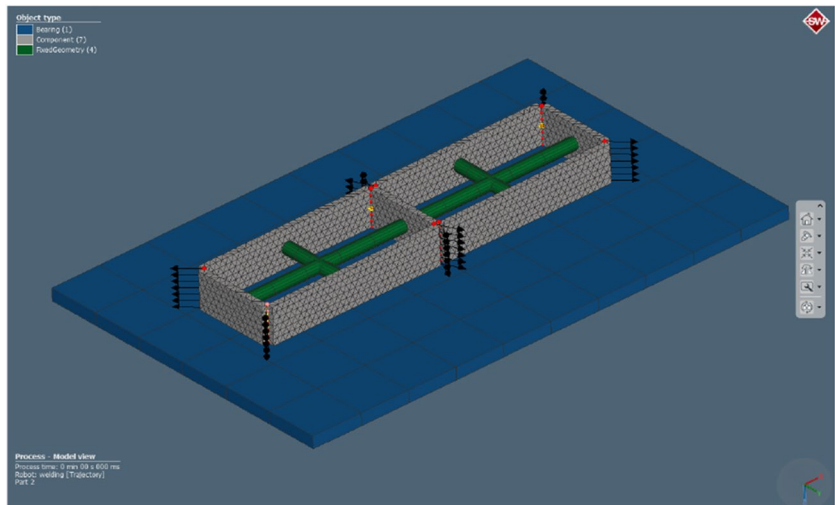


Table 1 UCL_{MR} for the width of the eye throughout welding processes [mm]

UCL_{MR} for the width w of the eye [mm]						
Flat bar	After welding operation I		After welding operation II		After welding operation III	
	Front	Rear	Front	Rear	Front	Rear
“K”	0.15756	0.241593	0.264654	0.289637	0.300619	0.467812

Table 2 UCL_{MR} for the height of the eye throughout welding processes [mm]

UCL_{MR} for the height h of the eye [mm]						
Flat bar	After welding operation I		After welding operation II		After welding operation III	
	Front	Rear	Front	Rear	Front	Rear
“P”	0.291135	0.125464	0.188058	0.171312	0.206178	0.210845

deformations, which are sensitive to any input deformations and oversights. The only exception is the decrease in UCL_{MR} between the length of flat bar “P” and the subsequent height of the eye. This may indicate a more effective fixing of this dimension during the assembly.

Dimensions measured from the rear, according to the results, generally exhibit lower repeatability. This trend is not true only in the case of the width of the eye after welding operation III, where the dimension from the front turned out to be less repeatable. The UCL_{MR} value clearly increases after welding operation III, which may suggest greater challenges and variability at this specific stage of the process, or the occurrence of measurement errors due to improper caliper use.

Statistical Process Control provided significant information regarding deviations from standards and the quality of the entire process. The analysis of UCL_{MR} allowed us to identify trends and differences in the repeatability of

operations depending on the type of flat bar, dimension, and technological stage.

4.2 Results of non-contact measurements

The results provide valuable information regarding the deformations that occurred in the frames. Out of 11 frames, the results for 4 selected ones will be presented, which are considered the most representative. Screenshots of the results for each eye after welding operation I and welding operation II are included in Figs. 3, 4, 5, and 6.

Deformations increase after welding operation II. Their characteristic shape and direction are preserved. The initial deformation occurred after welding operation I, and after operation II, it is only intensified. However, except for this case, the effect resulting from further welding stresses is consistent with expectations.

Fig. 3 Cross-section of deformation of eyes in VXInspect. Frame 1 after operation I (up) and II (down)

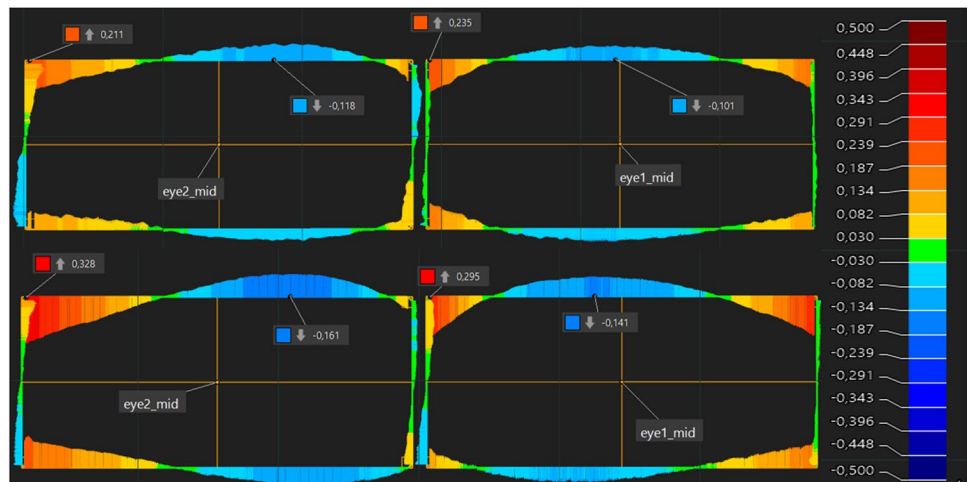


Fig. 4 Cross-section of deformation of eyes in VXInspect. Frame 6 after operation I (up) and II (down)

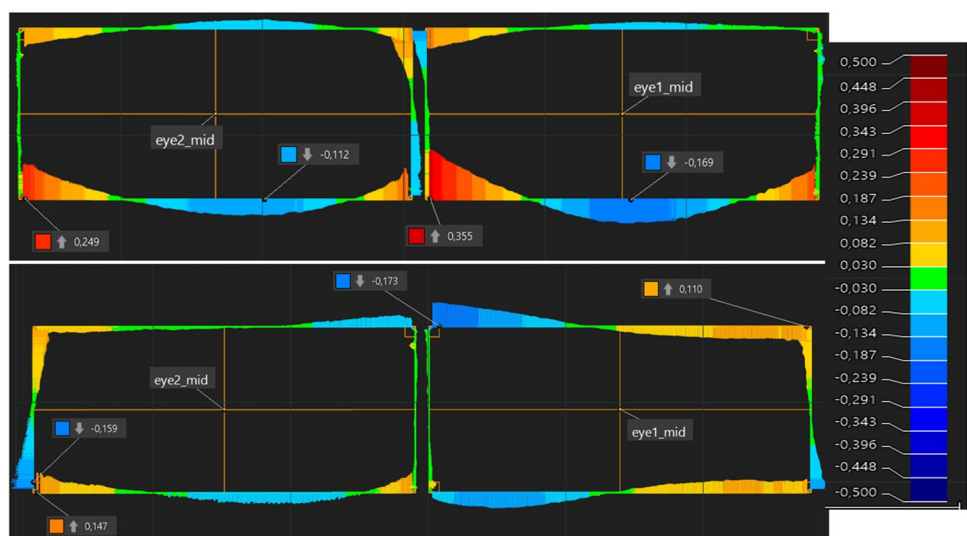


Fig. 5 Cross-section of deformation of eyes in VXInspect. Frame 10 after operation I (up) and II (down)

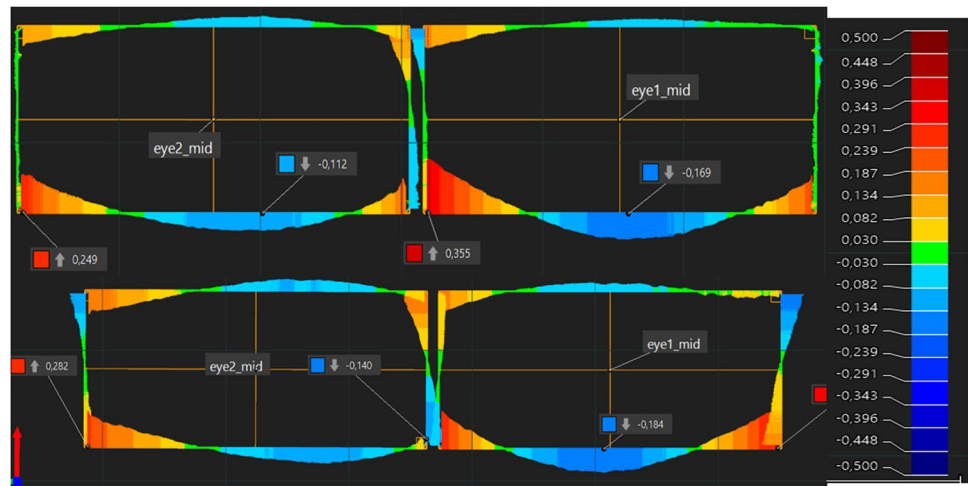
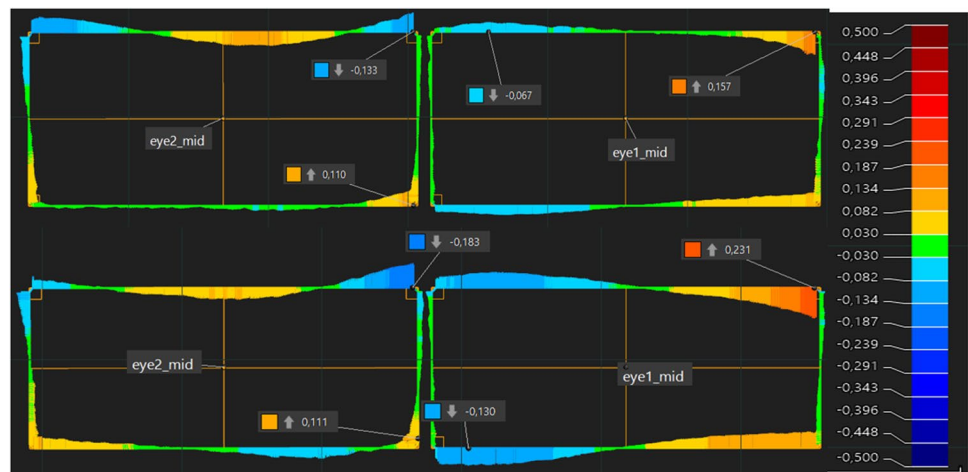


Fig. 6 Cross-section of deformation of eyes in VXInspect. Frame 11 after operation I (up) and II (down)



It is evident that in most cases, longer flat bars undergo significantly greater deformations. This directly affects the width dimension of the eye, whose repeatability in the case of type 1 frame was poor. It is worth noting that in the case of type 2, we are dealing with a longer flat bar; hence, the deformations are likely greater. Further research should be conducted for both frames in this regard. The occurrence of greater deformation for longer flat bars can be explained by two phenomena. Firstly, the larger dimension is directly related to greater initial deformations, occurring already after cutting. Secondly, the accompanying weld is longer, thus generating more intense stresses, further bending it. Faced with this phenomenon, the width of the eye, without proper preparation of the technology and consideration of greater accuracy in the production of longer flat bars, is doomed to flaws.

Comparing the directions of deformations of all frames allows us to notice that while there are certain tendencies, each is characterized by a different shape. This is particularly noticeable when comparing, for example, Fig. 3 with Fig. 4,

or Fig. 5 and Fig. 6. A common feature of each cross-section is that deformations increase at the corners. In addition, the bulges of longer flat bars are usually directed outwards, sometimes forming an “S” shape, as seen in Fig. 6. However, there is no particular repeatability, which confirms the conclusions drawn earlier from the analysis of measurements of type 1 frame. In this case, the technology also does not provide adequate quality or process stability.

Measurements using the 3D scanner allowed us to observe phenomena that would be impossible to capture with a caliper. They provided a comprehensive view of a specific feature. The lack of interoperative nominal dimensions remains a significant problem; however, even without them, the conducted inspection enables drawing reliable conclusions.

4.3 Results of the simulation in the Simufact Welding software

The results after cooling are presented in Figs. 7 and 8. At this stage, the maximum total deformation was 0.84 mm,

and the maximum stresses were 341.54 MPa. The Simufact Welding software also allowed obtaining values of total deformations in the normal direction, i.e., max. 0.74 and min. -0.64 mm. These values will be further compared to the results of actual deformation measurements.

The inspection was conducted on the same 11 scans of type 2 frames. Whereas previously it was carried out without nominal data, now all elements will be compared to the assembly of flat bars. The most important data extracted from the report, the maximum and minimum results from

the deformation map, have been summarized in the chart in Fig. 9 for each frame from no. 1 to no. 11. The blue colors represent the actual deformations that occurred in the examined frames. The orange and yellow lines indicate the respective range of the maximum and minimum values, thus representing the boundaries determined by the simulation in the Simufact Welding software.

The actual deformations exceed the theoretical calculations by more than double. This indicates the presence of disturbing factors that increase the intensity of deformation,

Fig. 7 Simufact Welding—the simulation results after cooling. Map of total deformations (× 10)

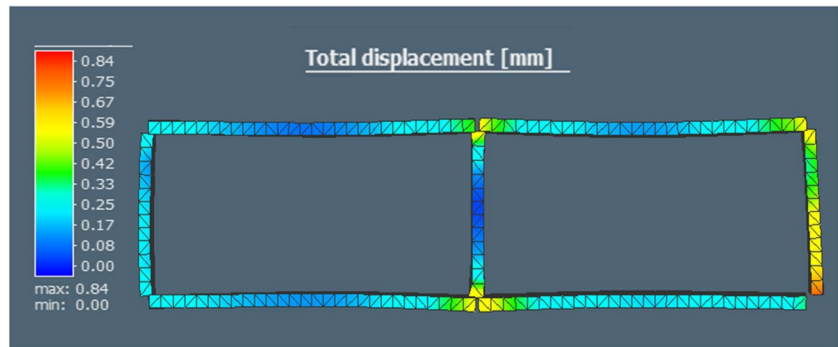


Fig. 8 Simufact Welding—the simulation results after cooling. Map of equivalent stresses

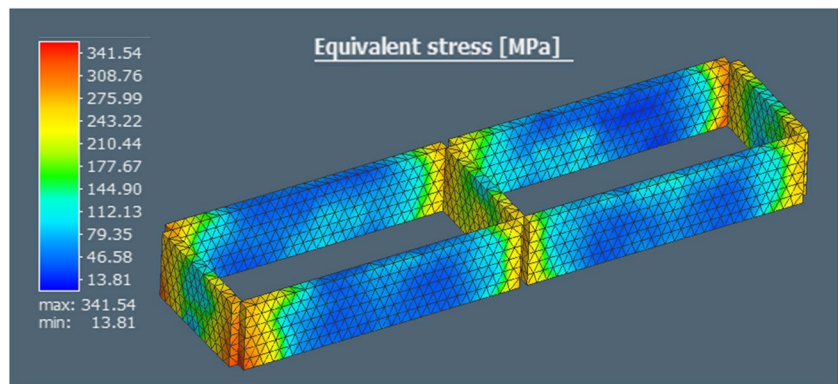
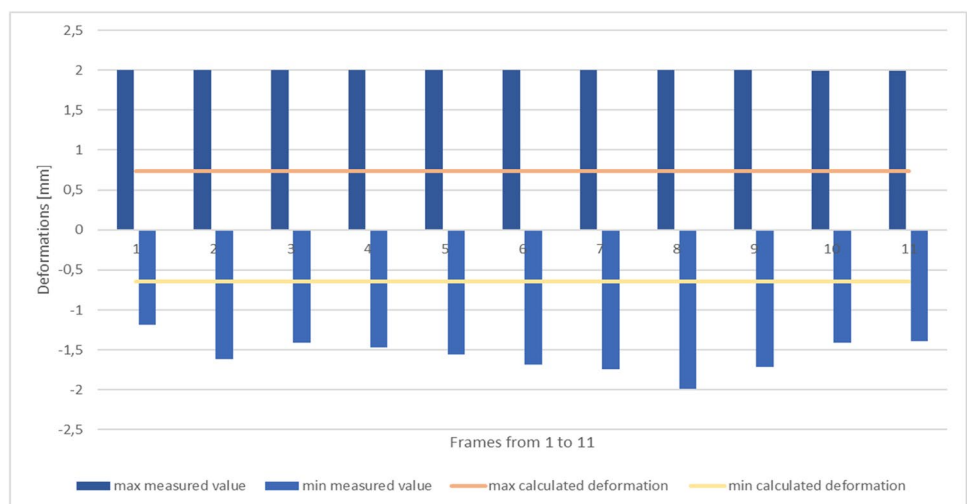


Fig. 9 Column chart of actual deformations for frames from no. 1 to no. 11



originating from sources other than the welding process itself. These are most likely pre-existing deformations in the longer flat bars or insufficient accuracy during the assembly of the elements onto the frame. This indicates the need for thorough quality control at every stage of element preparation, including the pretreatment stage.

5 Discussion and conclusions

To complete a similar task two measurement methods were applied: contact and non-contact; yet, the potential of the 3D scanner is incomparably greater. However, this does not diminish the areas where a caliper will remain useful.

In the case of a significantly reduced range of required dimensions, even the scanning itself proved to be longer. Additionally, the subsequent time-consuming process is processing the results in VXELEMENTS software. Thus, a manual scanner will not serve as a tool for quickly performing single measurements. In such cases, a regular caliper would be more suitable.

A 3D scanner enables the digitization of the entire product. After completing the scans of the examined objects, decisions regarding checking dimensions other than those assumed at the outset can be made at any time. Changing the approach to the inspection process may yield new, unexpected results. The ability to conduct a full dimensional and shape inspection would be particularly effective when compared to a CAD model. In such a scenario, the software would also consider the tolerances assumed in the project and indicate the most problematic areas. Such inspections guarantee easier identification of the sources of deviations.

Comparing theoretical deformations obtained through simulation in the Simufact Welding software with actual values measured using the HandySCAN 700 Elite device expanded the area of the conducted research. This analysis provided a proposed solution in the absence of an interoperable nominal model, and it proved effective in that role. Comparing the results revealed errors and narrowed the area of investigating the causes of excessive deformation. In most cases, longer flat bars undergo significantly greater deformations. A common feature of each cross-section was that deformations increased at the corners. In addition, the bulges of longer flat bars were usually directed outwards, sometimes forming an “S” shape. The actual deformations exceed the theoretical calculations by more than double.

Further studies may involve examining the impact of specific factors on the obtained results. It would be worthwhile, for example, to verify the effect of the sequence of laying welds. An interesting experiment could involve assembling 3D models of scanned flat bars and then performing theoretical simulations on them in Simufact Welding and actual welding processes, followed by scanning the frames. Such

a study would enable the verification of the influence of another significant factor, which is likely the initial deformation of the flat bars.

Combining 3D scanning methods with other technologies further expands the area of their applications. Integrating these tools can result in promising outcomes in scientific research and industrial applications. Using scanned data in combination with computer simulations allows for a more precise and complex analysis of objects from both theoretical and practical perspectives. As a result, combining these technologies may prove to be an effective method of improving existing technological solutions.

Acknowledgements We thank Dr. Aleksandra Świerczyńska from Gdańsk University of Technology, Institute of Manufacturing and Materials Technology, for invaluable guidance during preparing the simulation in Simufact Welding software.

We thank Mr. Krzysztof Braun from Gdańsk University of Technology, Institute of Manufacturing and Materials Technology, for his help during the measurements using 3D scanners.

Author contribution Conceptualization: MJ, DG, MD, MC. Methodology: MJ, DG, MD, MC. Formal analysis and investigation: MJ, DG, MD, MC. Writing—original draft preparation: MJ, DG. Writing—review and editing: MJ, DG, MD, MC. Funding acquisition: MD, MC. Resources: DG, MD, MC. Supervision: DG, MD.

Funding This work is funded by the European Commission in the framework HORIZON-WIDERA-2021-ACCESS-03, project 101079398 “New Approach to Innovative Technologies in Manufacturing (NEPTUN).” Scanners were financed by GDAŃSK TECH CORE EDU FACILITIES, grant no. 23/2021/EDU “Laboratory of Additive Manufacturing Methods and Reverse Engineering.”

Data availability The data that support the findings of this study are available from the corresponding author, [MD], upon reasonable request.

Declarations

Ethical approval All experimental protocols were approved by the management board of Base Group Sp. z o.o.

Guideline statement All methods were carried out in accordance with relevant guidelines and regulations.

Consent statement Informed consent was obtained from all subjects and their legal guardians.

Competing interest The authors declare no competing interests.

Open Access This article is licensed under a Creative Commons Attribution 4.0 International License, which permits use, sharing, adaptation, distribution and reproduction in any medium or format, as long as you give appropriate credit to the original author(s) and the source, provide a link to the Creative Commons licence, and indicate if changes were made. The images or other third party material in this article are included in the article’s Creative Commons licence, unless indicated otherwise in a credit line to the material. If material is not included in the article’s Creative Commons licence and your intended use is not permitted by statutory regulation or exceeds the permitted use, you will

need to obtain permission directly from the copyright holder. To view a copy of this licence, visit <http://creativecommons.org/licenses/by/4.0/>.

References

- Ratá V, Secobeanu S (2019) Aspects of using 3-d laser scanning technology in ship retrofit projects: annals of “Dunarea de Jos” University of Galati. Fascicle XI Shipbuild 42:157–162
- Szelewski M, Wieczorowski M (2015) Reverse engineering and methods of discretization of physical objects. *Mechanik* 12:183–188
- Koelman HJ (2010) Application of a photogrammetry-based system to measure and re-engineer ship hulls and ship parts: an industrial practices-based report. *Comput Aided Des* 42:731–743
- Liu L, Cai H, Tian M, Liu D, Cheng Y, Yin W (2023) Research on 3D reconstruction technology based on laser measurement. *J Braz Soc Mech Sci Eng* 45(6):1–20
- Wirza R, Sangaralingam K, Beng NS (2006) Complex shape measurement using 3D scanner. *Jurnal Teknologi* 45:97–112
- Raja V, Fernandes KJ (2007) Reverse engineering: An industrial perspective. Springer
- Gapinski B, Wieczorowska M, Marciniak-Podsadna L, Dybala B, Ziolkowski G (2014) Comparison of different method of measurement geometry using CMM, optical scanner and computed tomography 3d. *Proc Eng* 69:255–262
- Mendřický R, Langer O (2019) Influence of the material on the accuracy of optical 3D digitalization. *MM Sci J* 2783–2789. https://doi.org/10.17973/MMSJ.2019_03_2018121
- Muminović AJ, Smajić J, Šarić I, Pervan N (2023) 3D Scanning in Industry 4.0. *Basic Technol Model Implement Ind* 4:231–240
- Roca-Pardiñas J, Ordóñez C, Cabo C, Menéndez-Díaz A (2017) Assessing planar asymmetries in shipbuilding from point clouds. *Measurement* 100:252–261
- Ebrahim MAB (2015) 3D laser scanners’ techniques overview. *Int J Sci Res* 4(10):323–331
- Deja M, Dobrzyński M, Rymkiewicz M (2019) Application of reverse engineering technology in part design for shipbuilding industry. *Pol Marit Res* 26(2):126–133
- Kanun E, Yakar M (2021) Mobile phone-based photogrammetry for 3D modeling of ship hulls. *Mersin Univ J Marit Fac* 3(1):9–16
- Kanun E, Kanun GM, Yakar M (2022) 3D modeling of car parts by photogrammetric methods: example of brake discs. *Mersin Photogramm J* 4(1):7–13
- Son K, Lee WS, Lee KB (2021) Effect of different software programs on the accuracy of dental scanner using three-dimensional analysis. *Int J Environ Res Public Health* 18(16):8449
- Wersényi G, Scheper V, Spagnol S, Eixelberger T, Wittenberg T (2023) Cost-effective 3D scanning and printing technologies for outer ear reconstruction: Current status. *Head Face Med* 19(1):46
- Helle RH, Lemu HG (2021) A case study on use of 3d scanning for reverse engineering and quality control. *Mater Today: Proc* 45:5255–5262
- Ghahremani K, Safa M, Yeung J et al (2015) Quality assurance for high-frequency mechanical impact (HFMI) treatment of welds using handheld 3D laser scanning technology. *Weld World* 59:391–400
- Aminzadeh A, Karganroudi SS, Barka N, El Ouafi A (2021) A real-time 3D scanning of aluminum 5052–H32 laser welded blanks; geometrical and welding characterization. *Mater Lett* 296:129883
- Bologna F, Tannous M, Romano D, Stefanini C (2022) Automatic welding imperfections detection in a smart factory via 2-D laser scanner. *J Manuf Process* 73:948–960
- Niederwanger A, Warner DH, Lener G (2020) The utility of laser scanning welds for improving fatigue assessment. *Int J Fatigue* 140:105810

Publisher's Note Springer Nature remains neutral with regard to jurisdictional claims in published maps and institutional affiliations.